© 2015. Published by The Company of Biologists Ltd | Development (2015) 142, 438-443 doi:10.1242/dev.113571

RESEARCH REPORT

STEM CELLS AND REGENERATION

Tetraspanin CD9 and ectonucleotidase CD73 identify an osteochondroprogenitor population with elevated osteogenic properties

Anju Singh[1,*], Chantel Lester[2], Rebecca Drapp[3], Dorothy Z. Hu[4], Laurie H. Glimcher[5,*] and Dallas Jones[6]

ABSTRACT

Cell-based bone regeneration strategies offer promise for traumatic bone injuries, congenital defects, non-union fractures and other skeletal pathologies. Postnatal bone remodeling and fracture healing provide evidence that an osteochondroprogenitor cell is present in adult life that can differentiate to remodel or repair the fractured bone. However, cell-based skeletal repair in the clinic is still in its infancy, mostly due to poor characterization of progenitor cells and lack of knowledge about their *in vivo* behavior. Here, we took a combined approach of high-throughput screening, flow-based cell sorting and *in vivo* transplantation to isolate markers that identify osteochondroprogenitor cells. We show that the presence of tetraspanin CD9 enriches for osteochondroprogenitors within $CD105^+$ mesenchymal cells and that these cells readily form bone upon transplantation. In addition, we have used Thy1.2 and the ectonucleotidase CD73 to identify subsets within the $CD9^+$ population that lead to endochondral or intramembranous-like bone formation. Utilization of this unique cell surface phenotype to enrich for osteochondroprogenitor cells will allow for further characterization of the molecular mechanisms that regulate their osteogenic properties.

KEY WORDS: Osteochondroprogenitor, Osteoblast, Skeletal stem cell

INTRODUCTION

Bone formation during embryonic development and postnatal life is a tightly regulated biological process (Olsen et al., 2000). During embryonic development cells of the mesenchymal lineage migrate to specific anatomical locations and either directly differentiate to bone-forming osteoblasts by intramembranous ossification or form bone via a cartilaginous scaffold by endochondral ossification (Karsenty and Wagner, 2002; Kronenberg, 2003). The differentiation of osteoblasts or chondrocytes from a common osteochondroprogenitor is extremely complex and relies on the expression of various transcriptional regulators and growth factors (Karsenty, 2008).

Evidence exists that an osteochondroprogenitor cell can replenish post-mitotic osteoblasts in adults during bone remodeling or injury as well as cartilage after bone marrow stimulation techniques such as microsurgery (Otsuru et al., 2008; Maes et al., 2010). However, controversies exist regarding the identity of these osteochondroprogenitor cells, and this issue remains a challenge for wide clinical application of these cells in bone and cartilage repair (Bianco et al., 2008; Robey, 2011; Mobasheri et al., 2014). To date, molecular characterization of osteochondroprogenitor cells has been fairly limited, owing to a lack of definitive markers to reliably identify and characterize these cells. Traditionally, cultures of mesenchymal progenitors are derived from bone marrow or neonatal calvariae and consist of cells with diverse replicative age and differentiation potential, leading to the observed phenotypic and functional heterogeneity in these cultures (Goshima et al., 1991; Bianco et al., 2010; Bakker and Klein-Nulend, 2012). Moreover, these cultures are often contaminated by hematopoietic cells and fibroblasts. Hence, the ability to purify subpopulations of various lineages that contribute to bone formation *in vivo* would enhance our understanding of the molecular mechanisms that regulate this physiological process.

Initial studies that sought to purify these populations through immunophenotyping demonstrated that cell-surface markers like CD146 and CD105 can be used to enrich for cells with osteogenic properties (Sacchetti et al., 2007; Chan et al., 2009). Additional studies demonstrated that the $CD105^+$ cell population is heterogeneous and can be further subdivided based on expression of Thy1 (also termed CD90) (Chan et al., 2009). Likewise, recent studies have shown that an $Mx\text{-}1^+$ (Mx1 – Mouse Genome Informatics) population of cells has multilineage potential *in vitro*; however, these cells were osteolineage restricted *in vivo* (Park et al., 2012). Thus, additional characterization of the cell surface markers present on these mesenchymally derived progenitor cells is still necessary to allow for a greater enrichment and characterization of the cells that give rise to osteoblasts and chondrocytes.

In this study, we have used a combination of high-throughput screening, flow cytometry-based cell sorting and further *in vitro* and *in vivo* characterization to identify a panel of cell surface markers that can be used to isolate osteochondroprogenitor cells. We show that CD9 is expressed on a fraction of $CD105^+$ cells that enriches for cells that exhibit marked expression of osteochondro-lineage genes and are capable of robust bone formation when transplanted *in vivo*. In addition, we have identified subsets among the $CD9^+$ cells that lead to endochondral or intramembranous-like bone formation.

RESULTS AND DISCUSSION

Identification of CD9 as a marker for osteochondroprogenitors

We established a flow cytometry-based high-throughput antibody screen to identify cell surface markers that can be used to isolate osteochondroprogenitor cells. Fetal bone suspensions from wild-type embryos at E16.5 were stained with a panel of antibodies that have previously been reported to identify mesenchymally derived progenitor cells ($CD45^-Ter119^-Tie2^-CD105^+$) and are referred to

[1]Department of Preclinical Innovation, National Center for Advancing Translational Sciences, National Institutes of Health, Rockville, MD 20850, USA. [2]Division of Rheumatology, Brigham and Women's Hospital, Boston, MA 02115, USA. [3]College of Veterinary Medicine, North Carolina State University, Raleigh, NC 27607, USA. [4]Endocrine Unit, Massachusetts General Hospital, Boston, MA 02114, USA. [5]Department of Medicine, Weill Cornell Medical College, New York, NY 10065, USA. [6]Abide Therapeutics, San Diego, CA 92121, USA.

*Authors for correspondence (anju.singh@nih.gov; lglimche@med.cornell.edu)

Received 5 June 2014; Accepted 28 November 2014

Development (2015) 142, 438-443 doi:10.1242/dev.113571

as CD105$^+$ from hereon (Chan et al., 2009). We screened >250 antibodies to further characterize the CD105$^+$ cells and identified 31 markers that were present on CD105$^+$ cells (supplementary material Fig. S1). One cell surface marker of potential interest was CD9, a member of the tetraspanin superfamily that has been reported to function as organizer of multimolecular membrane complexes by recruiting proteins into tetraspanin-enriched microdomains (TEM) (Boucheix and Rubinstein, 2001). Tetraspanins regulate diverse biological processes, including membrane fusion, cell adhesion and migration, cancer and viral infections (Yanez-Mo et al., 2009). It has been shown that CD9 is upregulated in the osteoarthritic synovial lining layer, where it might affect pathogenesis of osteoarthritis by facilitating formation of signaling complexes (Korkusuz et al., 2005). Another study reported that progenitor cells isolated from human osteoarthritic cartilage express CD9 (Fickert et al., 2004). Interestingly, CD9 has recently been used to dissect functional heterogeneity within the hematopoietic stem cell compartment (Karlsson et al., 2013), and we postulated that it might also do so in the mesenchymal stem cell (or bone marrow stromal cell) compartment.

CD9 was expressed on 25% of the CD105$^+$ cells at E16.5 (Fig. 1A) and was also expressed on the surface of a transformed mouse osteoblast clone, human bone marrow stromal cells and on human embryonic bone marrow stromal cells (supplementary material Fig. S2). We next employed flow cytometry to isolate CD105$^+$CD9$^+$ (referred as CD9$^+$) and CD105$^+$CD9$^-$ (referred as CD9$^-$) cells from mouse embryonic limbs to analyze gene expression in these two cell populations. As shown in Fig. 1B, CD9$^+$ cells exhibited profoundly elevated levels of transcripts associated with chondrocyte and osteoblast lineage cells, including Sox9, collagen type 2 (Col2; Col2a1 – Mouse Genome Informatics), collagen type X (ColX; Col10a1 – Mouse Genome Informatics), Runx2, osterix (Osx; Sp7 – Mouse Genome Informatics), alkaline phosphatase [TNALP; alkaline phosphatase, liver/bone/kidney (Alpl) – Mouse Genome Informatics], osteopontin (OPN; Spp1 – Mouse Genome Informatics) and bone sialoprotein (BSP; Ibsp – Mouse Genome Informatics), when compared with CD9$^-$ cells. Furthermore, sorted CD9$^+$ cells readily differentiated to osteoblasts and chondrocytes when cultured under osteoblast- or chondrocyte-differentiating conditions *in vitro*, whereas the CD9$^-$ population did not mineralize or form cartilage (Fig. 1C-E). These data suggest that CD9 can be used as a cell surface marker in combination with CD105 to enrich for cells of the osteochondro lineage.

CD9$^+$ osteochondroprogenitors give rise to bone and cartilage *in vivo*

To establish the osteogenic potential of CD9$^+$ cells *in vivo*, we used a previously established (Chan et al., 2009) kidney capsule transplantation assay that utilizes micro-quantitative computed tomography (micro-QCT) to monitor bone formation. Equal numbers of sorted CD9$^+$ or CD9$^-$ were transplanted under the kidney capsule of recipient mice and kidneys were harvested six weeks post transfer for analysis. Micro-QCT and histological

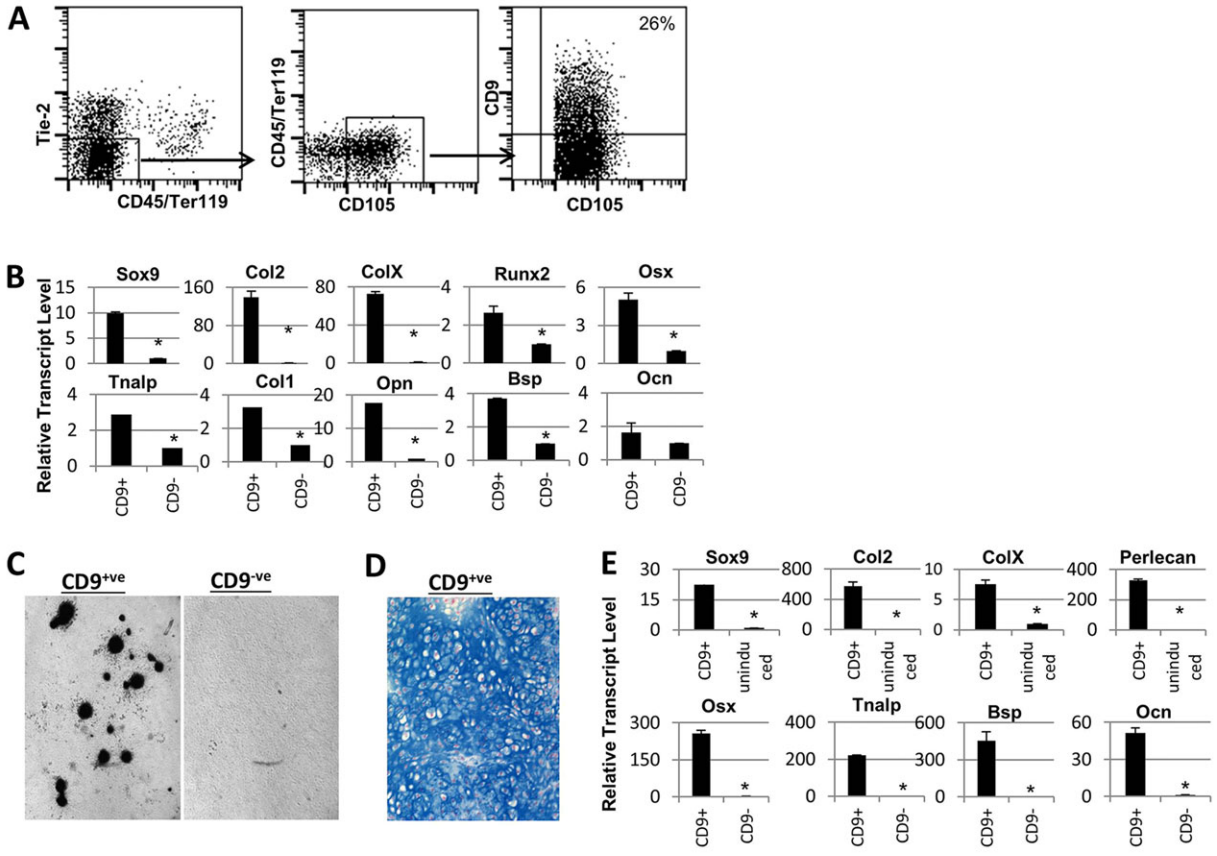

Fig. 1. Identification of CD9 as a marker for osteochondroprogenitors. (A) Representative flow plots of mice embryonic limb suspension at E16.5 stained with anti-CD45, anti-Ter119, anti-Tie2, anti-CD105 and anti-CD9. The dot plot on the right is pre-gated on CD45$^-$Tie2$^-$Ter119$^-$CD105$^+$ cells. (B) qPCR expression of the indicated transcripts in sorted CD9$^+$ or CD9$^-$ from E16.5 fetal limbs. (C) Von Kossa staining of sorted CD9$^+$ or CD9$^-$ cells from E16.5 fetal bones after 15 days in osteoblast differentiation media. (D) Toluidine Blue staining of section of chondrocyte pellet from sorted CD9$^+$ cells after 2 weeks in chondrocyte differentiation media. (E) qPCR expression of the indicated transcripts in chondrocyte pellets from sorted E16.5 CD9$^+$ cells after 2 weeks in chondrocyte-inducing conditions (top panel) or sorted E16.5 CD9$^+$ or CD9$^-$ after 2 weeks in osteoblast-differentiating conditions (bottom panel). *P<0.05; Student's t-test.

Development (2015) 142, 438-443 doi:10.1242/dev.113571

evaluation of donor kidneys revealed that the transferred $CD9^+$ cells readily gave rise to 40 times more bone than $CD9^-$ cells (Fig. 2A). $CD9^+$ cells were capable of forming bone with marrow cavity and supporting hematopoiesis (supplementary material Fig. S3). $CD9^+$ cells were also capable of giving rise to cartilage *in vivo* (Fig. 2B). To confirm that the donor cells were driving the *de novo* bone formation, we transferred $CD9^+$ progenitor cells isolated from GFP transgenic mice under the kidney capsule of non-GFP transgenic mice. Histological analysis revealed that the bone elements formed in the kidney capsule consisted of donor-derived GFP^+ cells, whereas the hematopoietic and vascular components were host derived (Fig. 2C).

Finally, we wanted to determine whether CD9 could be used to identify cells with osteogenic potential in an adult animal. To this end, we digested the long bones from adult mice and analyzed the cell surface profile of these cells. A small subset of $CD9^+$ cells were present among the $CD105^+$ cells in the adult mouse bone, demonstrating that CD9 can be used as a marker to identify osteochondroprogenitor cells in adult long bones (supplementary material Fig. S4). Thus, the elevated expression of osteochondro-lineage genes in combination with the augmented bone forming capacity of the $CD9^+$ cells confirms the utility of this cell surface protein to enrich for osteochondroprogenitors.

The cell surface marker Thy1.2 further sub-characterizes the $CD9^+$ osteochondroprogenitors

It has previously been reported that the cell surface protein Thy1.2 can be used to delineate $CD105^+$ cells into osteochondroprogenitor cells ($CD105^+Thy1.2^-$) and committed osteoblast lineage cells ($CD105^+Thy1.2^+$). We therefore sought to determine whether CD9 was differentially expressed in these two subsets. Interestingly, staining the $CD105^+$ cells with CD9 and Thy1.2 gave rise to four distinct cell populations (Fig. 3A). We therefore isolated and then transferred these four individual subsets of cells under the kidney capsule as previously described to evaluate their bone forming potential. As shown in Fig. 3B, the $CD9^+Thy1.2^-$ cells produced markedly more bone *in vivo* than the other three subsets, including the $CD9^-Thy1.2^-$ cells. $CD9^+Thy1.2^-$ cells formed bone via a cartilage intermediate and also formed a marrow cavity (Fig. 3; supplementary material Fig. S5). Among the $Thy1.2^+$ cells, the presence of CD9 led to a 100-fold enrichment in bone forming ability as well. Gene expression analysis of these four individual populations revealed that, whereas all four populations expressed a number of osteoblast-related genes, only the $CD9^+Thy1.2^-$ population expressed both osteoblast- and chondrocyte-related genes (Fig. 3C). Collectively, these data further demonstrate that CD9 is a key marker that can be used to further enrich for a population of cells that has osteogenic potential *in vivo*.

Further functional and genetic characterization of $CD9^+$ osteochondroprogenitor cells using the cell surface marker CD73

During our initial screening of potential markers to enrich for osteochondroprogenitors, we identified the ecto-5′-nucleotidase CD73 (Nt5e – Mouse Genome Informatics) as being highly expressed on $CD105^+$ cells. We therefore tested whether CD73 could be used to further characterize the $CD9^+$ osteochondroprogenitor cells described above. Indeed, we found that staining of the $CD9^+$ osteochondroprogenitor cells for CD73 and Thy1.2 identified additional subpopulations (Fig. 4A). For the sake of simplicity, we will refer to these four subpopulations as OCP1 ($CD73^+Thy1.2^-$), OCP2 ($CD73^-Thy1.2^-$), OCP3 ($CD73^-Thy1.2^+$) and OCP4 ($CD73^+Thy1.2^+$). To determine whether there were any functional differences between these subpopulations, we transplanted these four separate populations under the kidney capsule and monitored bone formation. Interestingly, the OCP4 population produced very little bone *in vivo*, whereas the other three subpopulations produced similar amounts of bone (Fig. 4B).

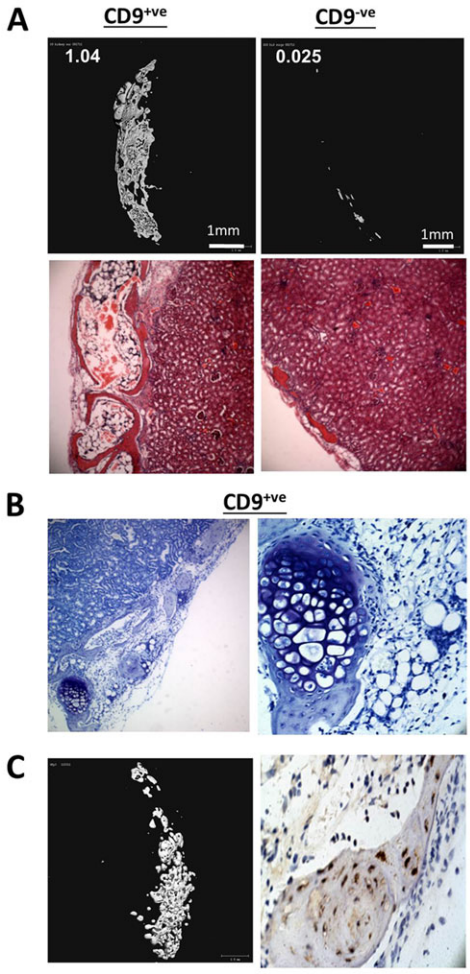

Fig. 2. $CD9^+$ osteochondroprogenitors give rise to bone and cartilage *in vivo*. (A) Representative 3D micro-CT images (upper panel) and H&E staining (lower panel) of kidneys transplanted with 20,000 sorted $CD9^+$ or $CD9^-$ cells. Kidneys were harvested 6 weeks post cell transfer and scanned using a micro-CT machine. The region of interest (ROI) was defined to include the entire kidney, and 2D image stacks were visually inspected to ensure that all heterotopic bone was included within the ROI. The numbers represent total bone volume in the ROI, calculated using built-in Scanco software. (B) Toluidine Blue staining of kidney sections 4 weeks after transplantation with 20,000 sorted $CD9^+$ or $CD9^-$ cells. (C) 20,000 sorted $CD9^+$ cells were transferred from GFP transgenic mice to non-transgenic mice. Kidneys were harvested 4 weeks post transplantation and were analyzed by micro-CT (left), or sections were immunostained against GFP (right).

Histological analysis of the bone produced by these various subpopulations revealed that the OCP1 population was able to give rise to bone that also contained marrow, whereas the marrow space was decreased in the OCP2 population and abolished in the OCP3 population. In addition to the different functional properties of these subpopulations to support marrow formation, we also sought to understand their genetic makeup, and therefore performed microarray analysis on these four FACS-sorted sub-populations. Differentially expressed genes between the various populations

Development (2015) 142, 438-443 doi:10.1242/dev.113571

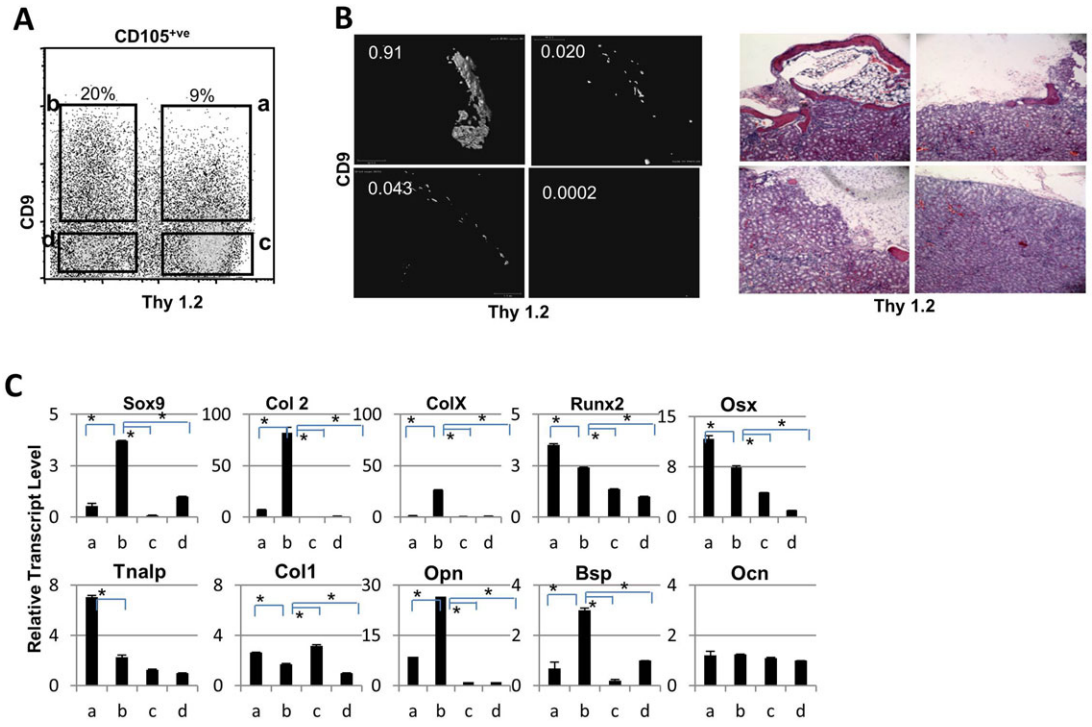

Fig. 3. The cell surface marker Thy1.2 further sub-characterizes CD9$^+$ osteochondroprogenitors. (A) Representative flow plot of mice embryonic limb suspension at E16.5 stained with anti-CD45, anti-Ter119, anti-Tie2, anti-CD105, anti-Thy1.2 and anti-CD9. The plot is pre-gated on CD105$^+$ cells. (B) Representative 3D micro-CT images (left) and H&E staining (right) of kidneys 6 weeks post transplantation with 20,000 sorted CD9$^+$Thy1.2$^+$, CD9$^+$Thy1.2$^-$, CD9$^-$Thy1.2$^+$ or CD9$^-$Thy1.2$^-$ E16.5 fetal bone cells. Numbers represent total bone volume calculated using micro-CT. (C) qPCR expression of indicated transcripts from sorted CD9$^+$Thy1.2$^+$ (a), CD9$^+$Thy1.2$^-$ (b), CD9$^-$Thy1.2$^+$ (c) or CD9$^-$Thy1.2$^-$ (d) E16.5 fetal bone suspension. *P<0.05; Student's t-test.

were identified using limma and were manually curated for any association with chondrocytes or osteoblasts. Detailed analysis of differentially expressed probes revealed that the OCP1 population expressed a higher level of genes associated with chondrocytes, including the transcription factors *Sox5*, *Sox6* and *Sox* 9 as well as *Col2*, aggrecan (*Acan* – Mouse Genome Informatics) and *Clec3a* (Fig. 4C,D). Interestingly, the expression of these chondrocyte-related genes was downregulated in the OCP2 population and even further decreased in the OCP3 and OCP4 populations. By contrast, the levels of genes associated with osteoblasts, such as *Osx* (Sp7), *Dlx5* and *Runx2*, were elevated in the OCP3 population. The OCP4 population that showed the lowest level of bone production *in vivo* also showed the lowest level of osteoblast- and chondrocyte-associated genes (Fig. 4C,D). Based on these data, we speculate that the OCP1 population is enriched for cells that have 'endochondral-like' potential and form bone via a cartilage intermediate, whereas the OCP3 might enrich for cells with an 'intramembranous-like' potential that do not go through a cartilage intermediate. However, we cannot rule out the possibility that these OCP1-4 populations might represent various stages of osteochondroprogenitor differentiation.

Collectively, the data we present in this paper demonstrate that the combination of cell surface staining for CD105, CD9, CD73 and Thy1.2 can identify unique populations of cells that possess unique gene signatures as well as distinct osteogenic potential *in vivo*. It will be of great interest to determine how these various subpopulations contribute to normal skeletal physiology during bone modeling and remodeling, as well as under pathogenic conditions that affect the skeleton. Furthermore, comprehensive characterization of these populations and the factors that regulate their differentiation and function will hopefully provide novel therapeutic targets that can promote bone and cartilage formation.

MATERIALS AND METHODS

Mice

Wild-type C57BL/6 mice were purchased from JAX and all mice were maintained and handled in accordance with guidelines by the Institutional Animal Care and Use Committee.

Isolation of embryonic and adult progenitor cells

Embryonic limbs (femur, tibia, humerus and radius) were dissected from the mouse embryos at E16.5 and digested with collagenase type 2 and dispase at 37°C for 45 min. After digestion samples were gently pipetted up and down to dissociate the cells and strained through a 70-µm cell strainer. The cells were pelleted and red blood cells were lysed using ammonium chloride, following which the cells were stained with fluorochrome-conjugated antibodies. For isolation of progenitor cells from adult long bones, skeletal elements were crushed gently using mortar and pestle after flushing the bone marrow and digested with collagenase and dispase for an hour at 37°C. The digest was pipetted up and down and strained, followed by red blood cell lysis.

High-throughput screening, cell sorting and *in vivo* transplantation

Flurochrome-conjugated antibodies were arrayed in a 96-well format (Biolegend), and the fetal cell suspension was resuspended in staining buffer (2% FBS in PBS) and stained with flurochrome-conjugated antibodies against CD45, Ter119, CD105, Thy1.2 and the test antibody for 30 min on ice. Samples were acquired using LSRII (BD Biosciences) and analyzed using FlowJo (TreeStar). For sorting, cells were re-suspended in αMEM supplemented with 10% FBS and sorted using FACS Aria II (BD

Development (2015) 142, 438-443 doi:10.1242/dev.113571

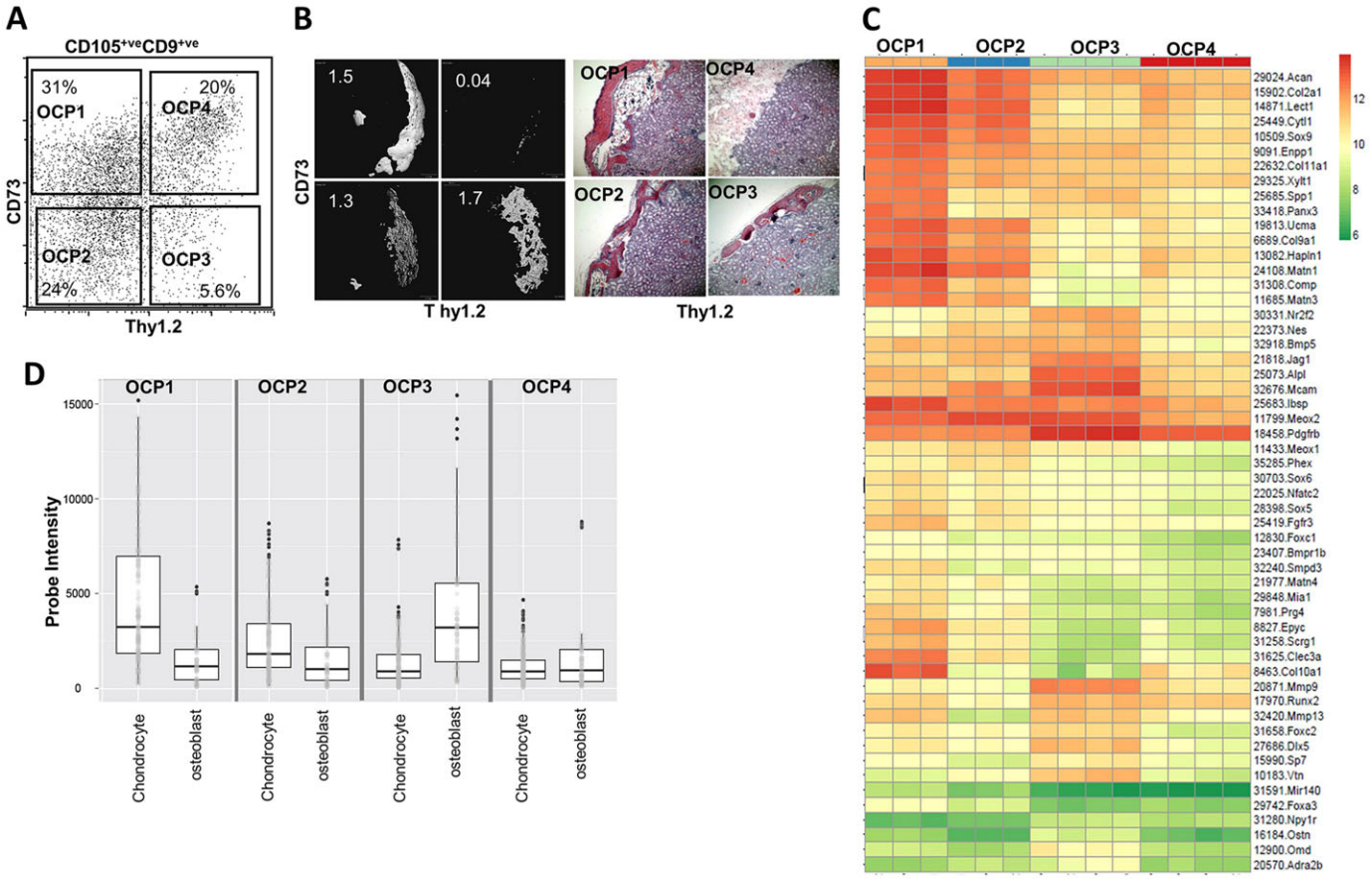

Fig. 4. The ecto-5′-nucleotidase CD73 further sub-characterizes the CD9$^+$ osteochondroprogenitors. (A) Dot plot showing staining with anti-CD73 and anti-Thy1.2 at E16.5. The plot is pre-gated on CD105$^+$CD9$^+$ cells. (B) Representative 3D micro-CT images and H&E staining of kidneys transplanted with 20,000 sorted OCP1 (CD73$^+$Thy1.2$^-$), OCP2 (CD73$^-$Thy1.2$^-$), OCP3 (CD73$^-$Thy1.2$^+$) and OCP4 (CD73$^+$Thy1.2$^+$) fetal bone suspension at E16.5. Kidneys were harvested 6 weeks post cell transfer. (C) Heat map showing genes differentially expressed between OCP1, OCP2, OCP3 and OCP4 fetal bone cells at E16.5. (D) Box plots demonstrating gene intensity expression between different populations. Differentially expressed genes were identified using limma and manually curated for any association with chondrocytes or osteoblasts.

Biosciences). Sorted cells were pelleted, washed with PBS, resuspended in 5 µl of matrigel and then transplanted underneath the kidney capsule of 8- to 12-week-old anesthetized male mice. Supplementary material Table S1 shows the number of transplants that were generated for each subpopulation of cells.

Micro-QCT analysis

Grafted kidneys were fixed overnight in 4% paraformaldehyde at 4°C. Micro-CT (Scanco Medical, µCT 35) was performed on fixed kidneys with an isotropic voxel size of 6 µm, an X-ray tube potential of 55 kVp, an X-ray intensity of 0.145 mA and an integration time of 600 ms, with a scan area that included the entire kidney. The region of interest (ROI) was defined to include the entire kidney, and two-dimensional (2D) image stacks were visually inspected to ensure that all heterotopic bone was included within the ROI. Analysis of bone volume within the ROI was performed using built-in Scanco software with segmentation parameters of 0.8/1/220 for support, sigma and threshold, respectively. Three-dimensional (3D) rendering was performed using built-in Scanco rendering software.

Osteoblast and chondrocyte differentiation

For osteoblast differentiation, sorted cells were cultured in αMEM and, once confluent, osteogenic differentiation was induced using osteogenic differentiation media (Lonza). For von Kossa staining of extracellular matrix mineralization, cells were fixed with 10% neutral buffered formalin and stained with a solution containing 2.5% silver nitrate (Sigma-Aldrich). For chondrogenic differentiation, the pellet cultures were established in polypropylene tubes according to instructions from Lonza. Pellets were fed with chondrogenic medium (Lonza) supplemented with TGF-β3 and were stained with Toluidine Blue after 2 weeks.

Histology

Engrafted kidneys were dissected and fixed in 4% paraformaldehyde in PBS for 24 h followed by decalcification with 15% tetrasodium EDTA for one week. Tissues were dehydrated in alcohol and xylene, embedded in paraffin and sectioned. For morphological analyses, tissue sections were stained with hematoxylin and eosin (H&E) or Toluidine Blue, or immunohistochemistry was performed using anti-GFP antibody (Abcam, ab 6556; 1:1000 dilution).

RNA isolation and quantitative real-time PCR

RNA was isolated from sorted cells using TRIzol (Invitrogen) or RNAeasy isolation kit (Qiagen), followed by reverse transcription with Affymetrix cDNA synthesis kit (Agilent) and real-time PCR using a Stratagene Mx3005.

Microarray

RNA was extracted from FACS sorted cells using RNeasy isolation kit (Qiagen). Microarray was performed using Mouse Gene 1.0 ST array at the Microarray Core Facility, Dana-Farber Cancer Institute (Boston, MA, USA). All MoGene 1.0 ST arrays were processed using the 'oligo' BioConductor package, quality-controlled with arrayQualityMetrics and corrected for batch effects with ComBat after RMA normalization. Differentially expressed genes were identified using limma. Data are available at GEO under accession number GSE64406.

Development (2015) 142, 438-443 doi:10.1242/dev.113571

Statistics

Statistical analysis was performed using two-tailed, unpaired Student's *t*-test. $P<0.05$ was considered significant.

Acknowledgements

We thank Marc Ferrer, Jae-Hyuck Shim, Julia Charles and Weiguo Zou for helpful discussions; Oliver Hofmann for help with the microarray analysis; Heather De Rivera and Kirsten Sigrist for technical support; and Deneen Kozoriz for help in cell sorting.

Competing interests

L.H.G. is on the Board of Directors and holds equity in Bristol Myers Squibb Pharmaceutical Company.

Author contributions

A.S. designed and performed experiments and prepared the manuscript. C.L., D.Z.H. and R.D. provided technical assistance with experiments. D.J. and L.H.G. supervised research, designed experiments and participated in manuscript preparation.

Funding

This work was supported by National Institutes of Health grants [HD055601 to L.H.G. and K99AR055668 to D.J.]. A.S. was supported by a fellowship from the Arthritis Foundation. Deposited in PMC for release after 12 months.

Supplementary material

Supplementary material available online at
http://dev.biologists.org/lookup/suppl/doi:10.1242/dev.113571/-/DC1

References

Bakker, A. D. and Klein-Nulend, J. (2012). Osteoblast isolation from murine calvaria and long bones. *Methods Mol. Biol.* **816**, 19-29.

Bianco, P., Robey, P. G. and Simmons, P. J. (2008). Mesenchymal stem cells: revisiting history, concepts, and assays. *Cell Stem Cell* **2**, 313-319.

Bianco, P., Robey, P. G., Saggio, I. and Riminucci, M. (2010). "Mesenchymal" stem cells in human bone marrow (skeletal stem cells): a critical discussion of their nature, identity, and significance in incurable skeletal disease. *Hum. Gene Ther.* **21**, 1057-1066.

Boucheix, C. and Rubinstein, E. (2001). Tetraspanins. *Cell. Mol. Life Sci.* **58**, 1189-1205.

Chan, C. K. F., Chen, C.-C., Luppen, C. A., Kim, J.-B., DeBoer, A. T., Wei, K., Helms, J. A., Kuo, C. J., Kraft, D. L. and Weissman, I. L. (2009). Endochondral ossification is required for haematopoietic stem-cell niche formation. *Nature* **457**, 490-494.

Fickert, S., Fiedler, J. and Brenner, R. E. (2004). Identification of subpopulations with characteristics of mesenchymal progenitor cells from human osteoarthritic cartilage using triple staining for cell surface markers. *Arthritis Res. Ther.* **6**, R422-R432.

Goshima, J., Goldberg, V. M. and Caplan, A. I. (1991). The osteogenic potential of culture-expanded rat marrow mesenchymal cells assayed in vivo in calcium phosphate ceramic blocks. *Clin. Orthop. Relat. Res.* **262**, 298-311.

Karlsson, G., Rörby, E., Pina, C., Soneji, S., Reckzeh, K., Miharada, K., Karlsson, C., Guo, Y., Fugazza, C., Gupta, R. et al. (2013). The tetraspanin CD9 affords high-purity capture of all murine hematopoietic stem cells. *Cell Rep.* **4**, 642-648.

Karsenty, G. (2008). Transcriptional control of skeletogenesis. *Annu. Rev. Genomics Hum. Genet.* **9**, 183-196.

Karsenty, G. and Wagner, E. F. (2002). Reaching a genetic and molecular understanding of skeletal development. *Dev. Cell* **2**, 389-406.

Korkusuz, P., Dagdeviren, A., Eksioglu, F. and Ors, U. (2005). Immunohistological analysis of normal and osteoarthritic human synovial tissue. *Bulletin* **63**, 63-69.

Kronenberg, H. M. (2003). Developmental regulation of the growth plate. *Nature* **423**, 332-336.

Maes, C., Kobayashi, T., Selig, M. K., Torrekens, S., Roth, S. I., Mackem, S., Carmeliet, G. and Kronenberg, H. M. (2010). Osteoblast precursors, but not mature osteoblasts, move into developing and fractured bones along with invading blood vessels. *Dev. Cell* **19**, 329-344.

Mobasheri, A., Kalamegam, G., Musumeci, G. and Batt, M. E. (2014). Chondrocyte and mesenchymal stem cell-based therapies for cartilage repair in osteoarthritis and related orthopaedic conditions. *Maturitas* **78**, 188-198.

Olsen, B. R., Reginato, A. M. and Wang, W. (2000). Bone development. *Annu. Rev. Cell Dev. Biol.* **16**, 191-220.

Otsuru, S., Tamai, K., Yamazaki, T., Yoshikawa, H. and Kaneda, Y. (2008). Circulating bone marrow-derived osteoblast progenitor cells are recruited to the bone-forming site by the CXCR4/stromal cell-derived factor-1 pathway. *Stem Cells* **26**, 223-234.

Park, D., Spencer, J. A., Koh, B. I., Kobayashi, T., Fujisaki, J., Clemens, T. L., Lin, C. P., Kronenberg, H. M. and Scadden, D. T. (2012). Endogenous bone marrow MSCs are dynamic, fate-restricted participants in bone maintenance and regeneration. *Cell Stem Cell* **10**, 259-272.

Robey, P. G. (2011). Cell sources for bone regeneration: the good, the bad, and the ugly (but promising). *Tissue Eng. Part B Rev.* **17**, 423-430.

Sacchetti, B., Funari, A., Michienzi, S., Di Cesare, S., Piersanti, S., Saggio, I., Tagliafico, E., Ferrari, S., Robey, P. G., Riminucci, M. et al. (2007). Self-renewing osteoprogenitors in bone marrow sinusoids can organize a hematopoietic microenvironment. *Cell* **131**, 324-336.

Yáñez-Mó, M., Barreiro, O., Gordon-Alonso, M., Sala-Valdés, M. and Sánchez-Madrid, F. (2009). Tetraspanin-enriched microdomains: a functional unit in cell plasma membranes. *Trends Cell Biol.* **19**, 434-446.

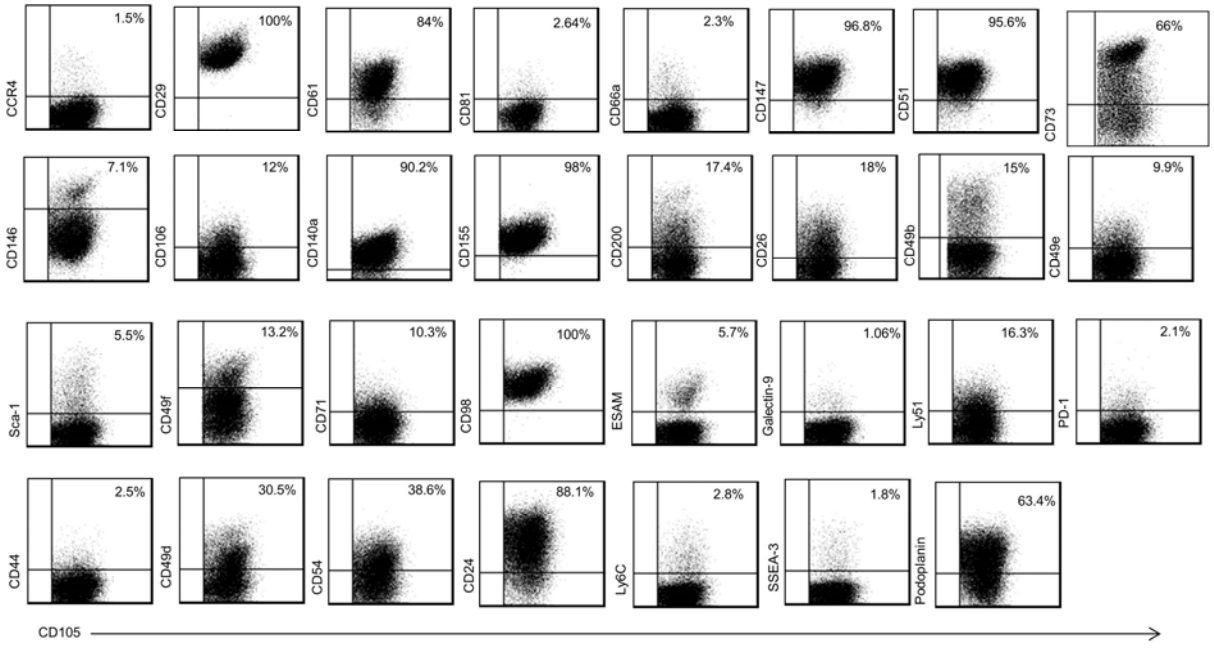

Figure S1: Markers expressed on CD105+ve cells at E16.5. Flow plots of mouse embryonic limb suspensions at E16.5 stained with anti-CD45, anti-Ter119, anti-Tie2, anti-CD105, and test antibody. The flow plots are pre-gated on CD45-veTer119-veTie2-veCD105+ve cells. The data is representative of two individual experiments.

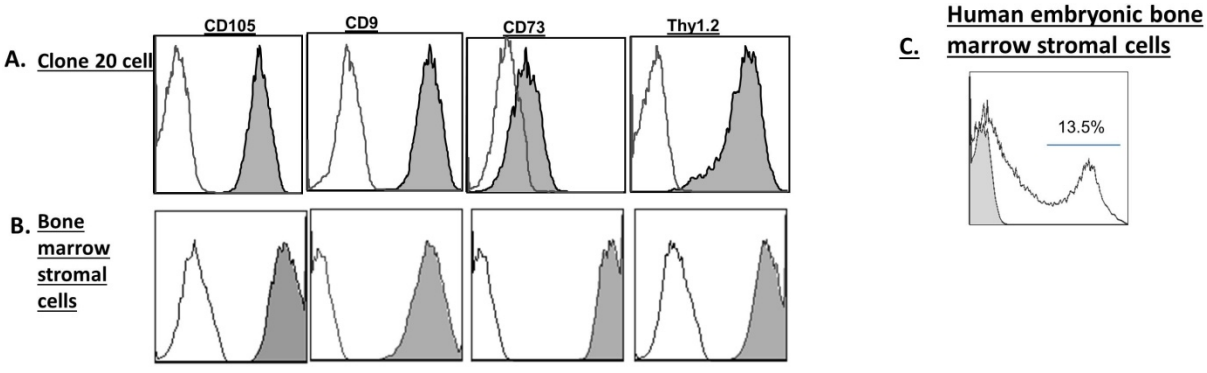

Figure S2: Expression of designated cell surface markers on cells from a transformed osteoblast clone, clone 20 (A) and human bone marrow stromal cells (B) and human bone marrow stromal cells isolated from femur of 19 week old embryos. (C). The unfilled plot in panel A and B and the filled histogram in panel C show the staining with isotype control.

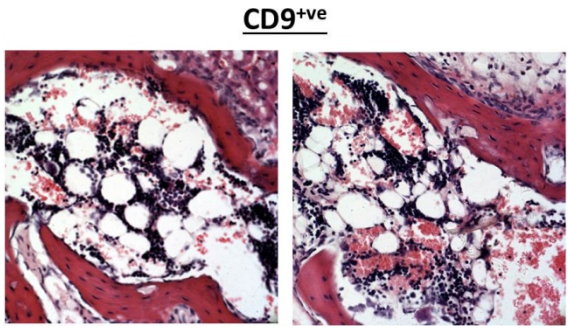

Figure S3: Haematoxylin and eosin staining of kidney sections transplanted with 20,000 sorted E16.5 CD9+ve cells. Kidneys were harvested 6 weeks post cell transfer.

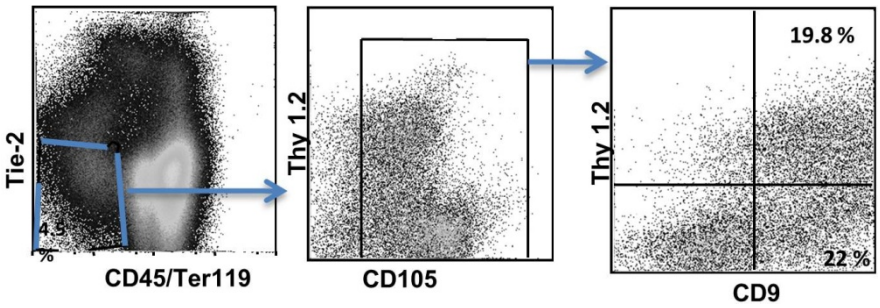

Figure S4: CD9+ve cells are present in adult mice. Femurs from 10 week old mice were digested with collagenase and dispase after flushing out the bone marrow and the cells were stained with anti-CD45, anti-Ter119, anti-Tie2, anti-CD105, anti-Thy1.2 and anti-CD9. The dot plot on the right is pre-gated on Tie2-ve CD45-veTer119-ve CD105+ve cells.

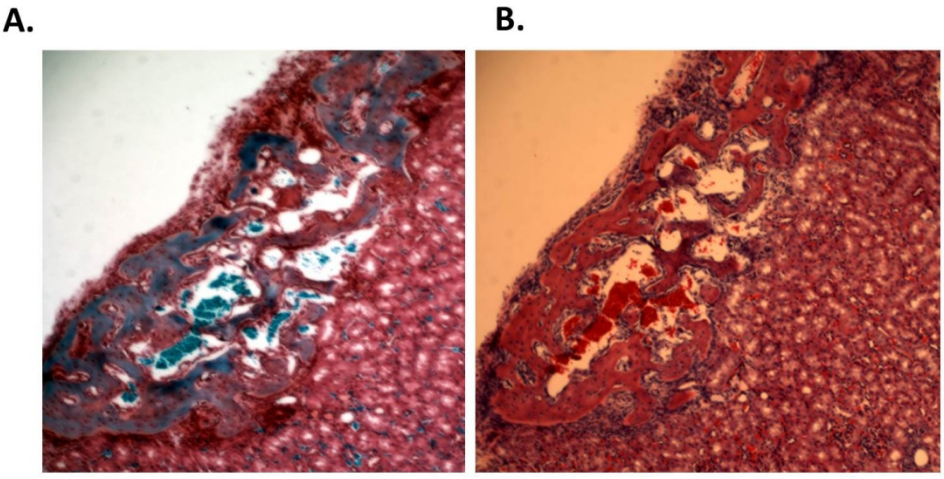

Figure S5: Safranin O (A) and H & E (B) stained section of kidney transplanted with 20,000 sorted CD9+ve Thy1.2-ve cells. Kidneys were harvested 16 days post cell transfer.

Table S1: The number of transplants undertaken for each population of cells and the number of transplants that generated bone with/without marrow.

	CD9+Thy1.2-		CD9+Thy1.2+		CD9+CD73+Thy1.2- (OCP1)		CD9+CD73-Thy1.2- (OCP2)		CD9+CD73-Thy1.2+ (OCP3)		CD9+CD73-Thy1.2+ (OCP4)	
16 days	Bone 3/3	marrow 1/3	Bone 1/2	marrow 0/2	Bone	marrow	Bone	marrow	Bone	marrow	Bone	marrow
4 weeks	2/2	1/2	2/2	0/2								
4.5 weeks	2/2	2/2	2/2	0/2								
6 weeks	6/6	6/6	6/6	0/6	8/8	8/8	7/7	6/7	7/7	1/7	0/8	0/8
8 weeks	8/8	8/8	3/3	0/3								